Size-Specific Concentration of DNA to a Nanostructured Tip Using Dielectrophoresis and Capillary Action

Woon-Hong Yeo,[†] Jae-Hyun Chung,*[,†] Yaling Liu,[‡] and Kyong-Hoon Lee[§]

Department of Mechanical Engineering, University of Washington, Box 352600, Seattle, Washington 98195, Department of Mechanical and Aerospace Engineering, University of Texas at Arlington, Box 19018, Arlington, Texas 76019, and NanoFacture, Inc., P.O. Box 52651, Bellevue, Washington 98015

Received: January 20, 2009; Revised Manuscript Received: April 29, 2009

One of the critical challenges in the fields of disease diagnostics and environmental monitoring is to concentrate extracellular DNA from a sample mixture rapidly. Unlike genomic DNA in normal cells, extracellular DNA dissolved in a biological sample can potentially offer crucial information about pathogens and toxins. The current concentration methods, however, are not able to directly concentrate extracellular DNA due to aggressive sample preparation steps. This paper presents a concentration mechanism of extracellular DNA onto a nanostructured tip using dielectrophoresis (DEP) in conjunction with capillary action. DNA immersed in a solution is captured onto a nanotip by two sequential actions: (1) attraction of DNA and other bioparticles in the vicinity of a nanotip by DEP and (2) size-specific capture of DNA onto the nanotip by capillary action. To investigate the size-specific capturing mechanism, an analytical model for the capillary action on a nanotip is presented, which is compared to the experiment for capturing polystyrene nanospheres. This analysis predicts the capture of a spherical particle smaller than 0.39 times a nanotip diameter, whereas our experiment shows that polystyrene spheres smaller than 0.84 times a nanotip diameter are captured. This discrepancy can be caused by the increase of the capturing force due to attractive DEP force. In addition, the diameter of the captured spheres can be increased by other experimental conditions including the tip geometry, the multiple particle interaction, and the contact angles. When a nanotip is used for concentrating λ-DNA, 6.7 pg/mL (210 aM) of DNA is selectively extracted from a sample mixture containing λ-DNA and Drosophila cells in one minute. The captured DNA is investigated by fluorescence microscopy, scanning electron microscopy (SEM), and X-ray analysis. This nanotip-based DNA concentrating method is a rapid and highly sensitive technique to detect extracellular DNA from a sample mixture.

1. Introduction

Extracellular DNA is of great interest in the fields of disease diagnostics and environmental molecular biology. Unlike the genomic DNA in normal cells, extracellular DNA is the free DNA released from dead cells. Thus, extracellular DNA circulating in body fluids can be used as an early indicator for various acute diseases such as cancer.[1,2] For example, the concentration of extracellular DNA for a normal person is ~30 ng/mL, but the concentration is increased to ~300 ng/mL for a cancer patient.[2] When the issue comes to environmental monitoring, extracellular DNA dissolved in lakes and soil is an indicator for environmental quality because the dissolved DNA is generated from cell lysis and excretion.[3,4]

In spite of such a great potential, the study of extracellular DNA is limited by the standard sample preparation methods. The conventional methods begin with filtering, centrifuging, and collecting DNA from a raw sample.[3−8] In aggressive experimental protocols, genomic DNA from normal cells is released and mixed with extracellular DNA. In addition, a few hours is required for the sample preparation process, which can degrade and mutate extracellular DNA.[6] As a result, the original information of extracellular DNA is partially or completely lost. Therefore, a rapid process that can concentrate extracellular DNA is very important for identifying pathogenic information.

This paper presents a size-specific concentration mechanism directly extracting extracellular DNA from a sample mixture using a nanostructured tip. The concentration process is performed with two sequences: (1) an alternating current (AC) electric field is applied to attract DNA and other bioparticles in the vicinity of a nanotip; (2) only the DNA is size-selectively captured onto the nanotip by the combination of dielectrophoresis and capillary action. In the analytical section, the forces involved in the concentration are estimated to investigate the capturing process. An analytical model is presented for capillary-induced size-selectivity that is described as the function of the ratio of a particle to a tip diameter. In experiment, polystyrene nanospheres are used to validate the size-specific capturing mechanism for nanotips. The capturing mechanism is finally demonstrated through DNA concentration from a sample mixture containing λ-DNA and Drosophila cells.

2. Size-Specific Concentration Mechanism

Figure 1(A) illustrates the DNA concentration process using an AC electric field and capillary action. To capture particles, a nanotip is immersed in a sample solution with an AC field. Under the inhomogeneous electric field, DNA or other particles in a medium are polarized and attracted to the tip by dielectrophoresis (DEP). When the tip is withdrawn from the solution, the attracted particles can be captured or released on the tip by

* To whom correspondence should be addressed. E-mail: jae71@u.washington.edu. Tel.: 1-206-543-4355. Fax: 206-685-8047.
[†] University of Washington.
[‡] University of Texas at Arlington.
[§] NanoFacture, Inc.

10.1021/jp900618t CCC: $40.75
Published on Web 07/10/2009

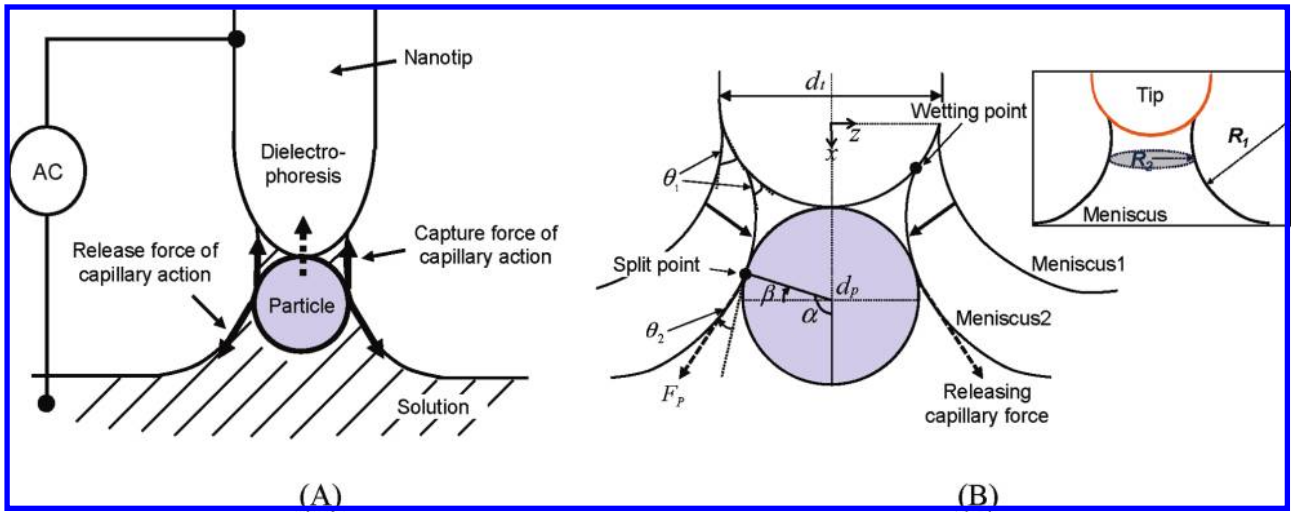

Figure 1. (A) DNA concentration process with DEP force (dotted arrow) and capillary forces (solid arrows). (B) Analysis for DEP and capillary forces.

combined effects of capillary action and DEP force. The DEP force attracts particles onto the tip, while the capillary forces can capture or release particles on the tip [Figure 1(A)]. To study the capturing process of a spherical particle, the magnitude of the DEP force is compared to that of the release force due to capillary action. The comparison predicts that the attractive DEP force is smaller than the release force. Subsequent analysis about capture and release capillary forces is performed to determine the capture of a spherical particle onto a nanotip.

2.1. Dielectrophoretic vs Releasing Capillary Forces. In the DNA concentration process shown in Figure 1(A), the DEP force acting on a spherical particle is proportional to the cubic diameter (d^3) of the spherical particle according to the Effective Dipole Moment (EDM) theory.[9] The theory suggests that as the particle diameter increases the corresponding DEP force is cubically increased. The EDM theory is based on the assumption that the electric field is not interfered by a particle because the characteristic dimension of a particle is negligibly small compared to that of an electric field. This assumption, however, is not valid for a particle whose diameter is comparable to a nanotip diameter because the electric field in the vicinity of a nanotip is significantly deformed by the presence of a particle.[10]

To precisely calculate the DEP force, the Maxwell Stress Tensor (MST) method is combined with the finite element method.[11] For the DEP force calculation, it is assumed that a polystyrene sphere (0−800 nm in diameter, d_p) suspended in pure water is attracted to a gold coated nanotip (d_t) having 500 nm in diameter as shown in Figure 1(B), and the sphere is in contact with the tip end. Because the geometrical errors of elements are generated between a sphere and a tip in the numerical analysis, the DEP force using this analysis is performed only for a particle diameter smaller than or equal to 800 nm. In this model, it is also assumed that the applied electric field does not generate electrokinetic flow and electric forces other than the DEP force. In the calculation, the dielectric constant and the conductivity of water are 80.1 and 0.001 S/m, respectively. The polystyrene spheres have the dielectric constant of 2.56 and the conductivity of 0.0011 S/m.[12]

The releasing capillary force is computed by considering the surface tension and the contact angle (θ_2) on a sphere [Figure 1(B)]. The surface tension force at the air−liquid interface is described as $F = L\gamma$, where L is the interfacial length between air and liquid and γ is the surface tension coefficient. According to the geometry as illustrated in Figure 1(B), the releasing capillary force (dotted line) is expressed as

$$F_p = (\pi d_p \cos\beta)\cdot\gamma\cos(\theta_2 + \beta) \quad (1)$$

where d_p is the diameter of the sphere; β is the angle between the horizontal line of the sphere and the radial line to the split point; and θ_2 is the contact angle at the sphere. At the split point, ($\pi d_p \cos\beta$) represents the interfacial length on the sphere.

According to eq 1, when $\beta = -\theta_2/2$, the maximum capillary force (F_{p_max}) is $\pi d_p\gamma\cos^2(\theta_2/2)$. Therefore, the capillary force is proportional to the diameter of a polystyrene sphere because of the surface tension. The maximum capillary force is computed for diameters (0−800 nm) of polystyrene spheres when the surface tension coefficient (γ) is 72.8 mN/m and the contact angle (θ_2) is 80°.[13]

Figure 2 compares the maximum releasing capillary force and the DEP force using the MST method. As the size of the polystyrene sphere increases, the capillary force and the DEP

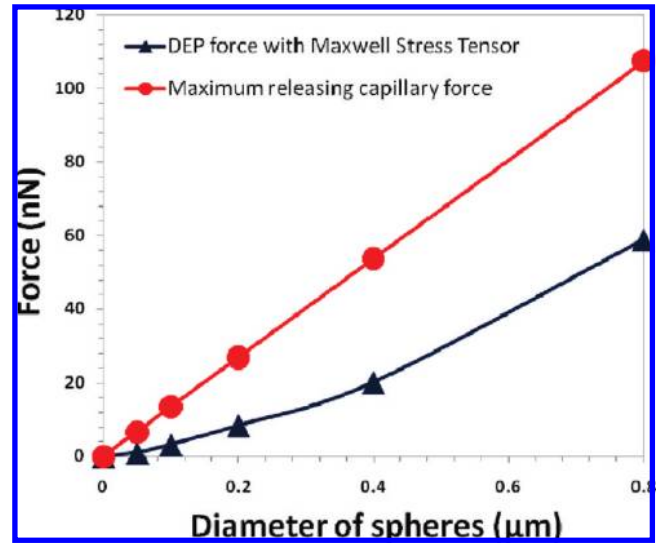

Figure 2. Comparison of the DEP force computed by the MST method and the maximum releasing capillary force according to the diameter of polystyrene spheres.

force elevate. The graphs represent that the sphere is always released from a nanotip because the releasing capillary force (red line with circles) acting on a sphere is greater than the DEP force (blue line with triangles). Thus, the subsequent analysis focuses on the comparison of the capturing and releasing capillary forces, which predicts whether a sphere is captured onto a nanotip.

2.2. Capturing vs Releasing Capillary Forces. As illustrated in Figure 1(A), a spherical particle in contact with a tip is exerted by capillary forces of two opposite directions when the sphere is withdrawn from a solution. A normalized diameter (d_n), the ratio of the particle diameter (d_p) to the tip diameter (d_t) [Figure 1(B)], is introduced to predict the capturing of a particle to a tip. As the tip is withdrawn from a solution, the meniscus profile at the tip is changed from the meniscus 1 to the meniscus 2 [Figure 1(B)]. During this withdrawal process, the contact angle (θ_1) is assumed to be constant at the tip surface. In this configuration, the general equation for the meniscus profiles is governed by the Young−Laplace equation,[14] $\Delta P = \gamma((1/R_1) - (1/R_2))$, where ΔP is the pressure difference between the air and the solution; R_1 is the radius of curvature in the $x-z$ plane; and R_2 is the radius of curvature in the perpendicular plane to the $x-z$ plane as illustrated in the inset of Figure 1(B). In the case of axi-symmetric structures,[15,16] $(1/R_1) = (d^2z/dx^2)/([1 + (dz/dx)^2]^{3/2})$ and $(1/R_2) = (dz/dx)/(x[1 + (dz/dx)^2]^{1/2})$. Therefore, for numerical computation, the Young−Laplace equation is described as

$$\frac{\Delta P}{\gamma} = \frac{d^2z/dx^2}{[1 + (dz/dx)^2]^{3/2}} - \frac{dz/dx}{x[1 + (dz/dx)^2]^{1/2}} \qquad (2)$$

When the diameter of the nanotip end is 500 nm, the size of the meniscus is in the range of a few micrometers. Since the diameter of the solution drop is much larger than the size of the meniscus, the solution is assumed to be a bulk liquid having an infinite diameter, thus $\Delta P/\gamma$ approaches zero. The meniscus profile on a tip can be estimated by eq 2 through numerical analysis. The contact angle on the tip surface [θ_1 in Figure 1(B)] is 51°. This angle is an average value of the contact angles measured by an optical microscope. The contact angle is used as the boundary condition for the numerical analysis.

As the withdrawal process of a tip continues, the meniscus 1 is changed to the meniscus 2 in Figure 1(B). When the meniscus 2 reaches the sphere surface, the split angle (α) and the split point are defined. At the split point, the solution is separated into the upper and lower parts. When α is greater than 90°, the particle stays in the solution [case (1) in Figure 3(A)]. When α is smaller than 90°, the particle is captured onto the tip [case (3) in Figure 3(A)]. At α of exactly 90° [case (2) in Figure 3(A)], the capture of a particle is not determined because the capturing and releasing capillary forces are the same. Through this analysis, a critical normalized diameter [$(d_n)_{critical}$] is defined at α = 90°. The $(d_n)_{critical}$ in the case (2) in Figure 3(A) is estimated by the numerical analysis of the meniscus profiles, which shows that the $(d_n)_{critical}$ is 0.39 [Figure 3(B)]. Therefore, as long as d_n is smaller than 0.39, the particle is captured onto a tip.

In this analysis, DEP force is not considered to calculate $(d_n)_{critical}$. If DEP force is added to the capillary forces, the $(d_n)_{critical}$ is increased because the capturing force of spheres is increased. In addition, the $(d_n)_{critical}$ is affected by the experimental conditions including the tip geometry, the multiple particle interaction, and the contact angle. These issues are discussed in the Experimental Section.

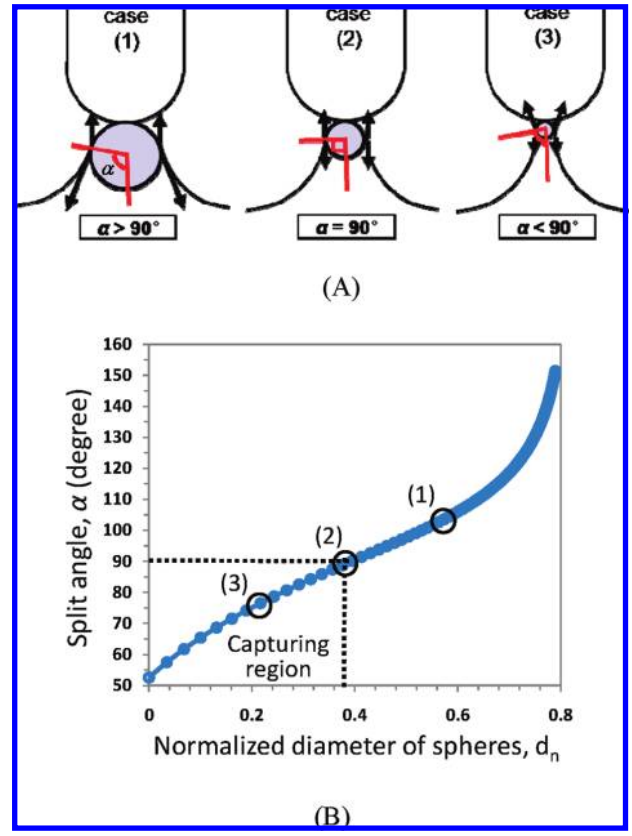

Figure 3. Size-selective capture of a spherical particle according to capillary action. (A) Split angle (α) variation according to the different sizes of a particle: case (1) shows when α > 90°, case (2) shows when α = 90°, and case (3) shows when α < 90°. (B) Variation of the split angles according to normalized diameters (d_n).

3. Experimental Section

3.1. Experimental Setup. The schematic of the experimental configuration is illustrated in Figure 4(A). An $x-y-z$ stage is utilized to control a nanotip that is used for capturing DNA in the axial direction. The capturing process is monitored by a microscope that is connected to a digital imaging system. Figure 4(B) shows the experimental setup including the $x-y-z$ stage under an optical microscope and an illuminator (MI-150, Dolan-Jenner, Lawrence, MA). During the capturing process, an AC electric potential is applied to the tip and the coil by a signal generator (Agilent 33220A, Santa Clara, CA).

3.2. Preparation of Nanotips. To fabricate a nanostructured tip, a one-dimensional fibril formation process was introduced.[17] Unlike the fibril composed only of single-walled carbon nanotubes (SWCNTs), the fabricated nanotip was composed of the mixture of SWCNTs and silicon carbide (SiC) nanowires. The fabrication of the hybrid nanotip began with dispersion of SWCNTs and SiC nanowires in separate vials. A weighed amount of SWCNTs (Carbon nanotechnologies, Inc., Houston, TX) was dispersed in dimethylformamide (DMF) by a sonicator (model 1510, Branson Ultrasonic Corp., Danbury, CT) for 10 h. The prepared SWCNT solution had the concentration of 100 mg/L. In the same way, SiC nanowires (Advanced Composite Materials Corporation, Greer, SC) were dispersed in DMF with the concentration of 200 mg/L. Each 5 mL of SWCNT and SiC nanowire solutions were mixed together and then sonicated for 1 h before use.

Note that a microtip was utilized to fabricate the nanotip. The microtip was made by using a gold-plated tungsten microwire (Sylvania, Towanda, PA) having 50 μm in diameter.

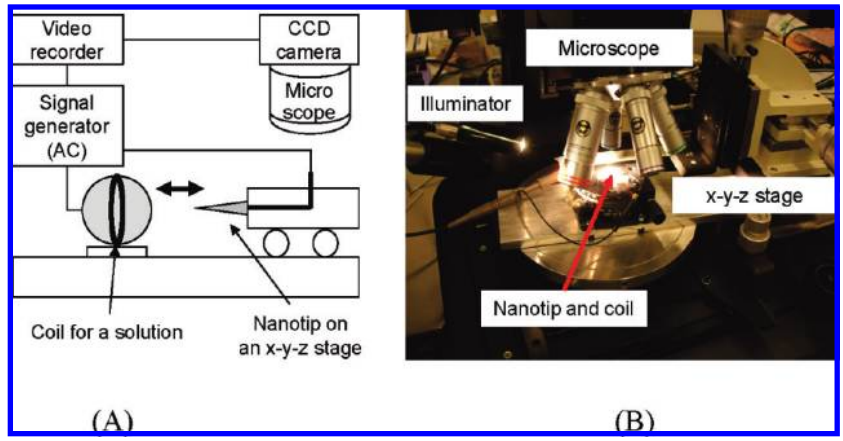

Figure 4. Experimental setup for DNA capture using a nanotip. (A) Schematic of the experimental setup. (B) Photo of the experimental setup.

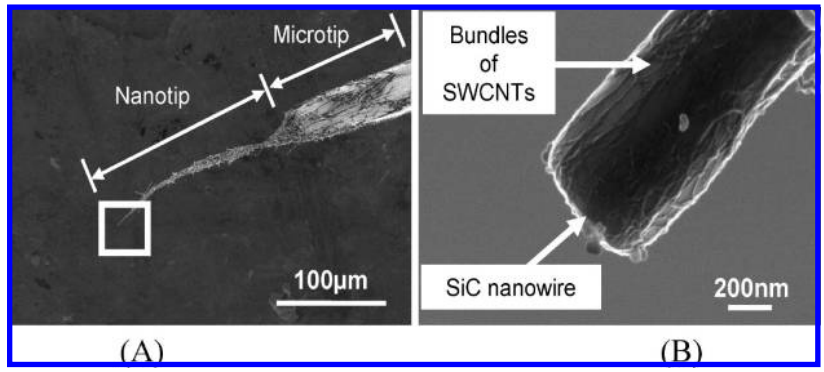

Figure 5. SEM images of a fabricated nanotip. (A) Nanotip fabricated on a microtip. (B) Magnified view of the tip end; a single SiC nanowire is wrapped by SWCNT bundles.

The microtip was prepared by cutting the wire with a paper trimmer or fracturing the wire by tension. For the nanotip fabrication, 2 μL of the SWCNT/SiC nanowire mixture was held in a silver-plated copper coil (OK industries, Tuckahoe, NY) by surface tension [Figure 4(A)]. Subsequently, the gold-plated tungsten microtip was immersed into the mixture with an AC potential (20 V_{pp} at 5 MHz; V_{pp} is peak-to-peak voltage). By withdrawing the microtip at a rate of 8 μm/s, a hybrid nanotip was fabricated.

Figure 5(A) shows an SEM image of a hybrid nanotip, while Figure 5(B) shows a SWCNTs-wrapped SiC nanowire at the end of the nanotip. Regarding the structure of the hybrid nanotip and its individual constituents, specific bindings (covalent or ionic) were not present for either of the crystal structures, but the highly flexible structure was formed by weaker interaction (van der Waals force). For the repetitive fabrication of nanotips, the lengths of the nanotips were controlled in the range of 200−400 μm. The tip fabrication process was controlled such that the nanotips could be ended with a single SiC nanowire. Therefore, the end diameter of a nanotip was determined by the diameter of the SiC nanowire at the end. This end diameter was important for the investigation of size-specific capture. Our SEM study showed that the average diameter and the standard deviation of the end diameters of the nanotips used in the experiment were 544 and 141 nm, respectively. Regarding the reproducibility, nanotips were successfully fabricated with a 90% yield over 100 attempts.

The polydimethylsiloxane (PDMS) coating process of a nanotip was developed to release the captured DNA from the tip surface and to avoid nonspecific binding between DNA molecules and SWCNTs. For instance, when DNA was captured onto a bare nanotip without PDMS coating, it was difficult to release the DNA in boiling water for repetitive use of the tip. However, when a PDMS-coated tip was used, the captured DNA could be released easily in boiling water. Thus, a nanotip with PDMS coating could be reused to capture and release DNA. Regarding the coating process, a bare nanotip was dipped into a PDMS solution with its curing agent at the ratio of 10:1 for 10 s. After withdrawal of the tip from the solution, the PDMS coated tip was cured at 60 °C for 1 h. Figures 6(A) and (B) show a nanotip coated with PDMS and the end of the nanotip, respectively. A uniform PDMS layer on the nanotip was 50 nm thick. Through this PDMS coating, the diameter of the tip was increased by 100 nm.

To test the robustness of the hybrid nanostructured tip, a bare nanotip and a PDMS-coated nanotip were repeatedly immersed in a buffer solution three times. The tip shape and morphology were inspected by an optical microscope and an SEM. Through the inspection, it was confirmed that both nanotip structures maintained their original shapes after repeated use.

To test electrical conductance of a nanotip without PDMS coating, two nanotips were connected to a junction by manipulating two tungsten microtips. Electrical conductance was measured between two nanotips through the junction. In the current−voltage measurement, the resistance of a 1.8 mm long hybrid fibril was ∼77 kΩ. Assuming a 400 μm long nanotip, the resistance of the fabricated nanotip was ∼17 kΩ. This resistance was low enough to attract DNA in a buffer solution. When a PDMS-coated nanotip was utilized to capture DNA, it showed similar capturing performance for DNA compared to a bare nanotip because a high frequency AC field (5 MHz) could pass through a 50 nm thick PDMS layer. It should be noted that the capturing performance was compared through fluores-

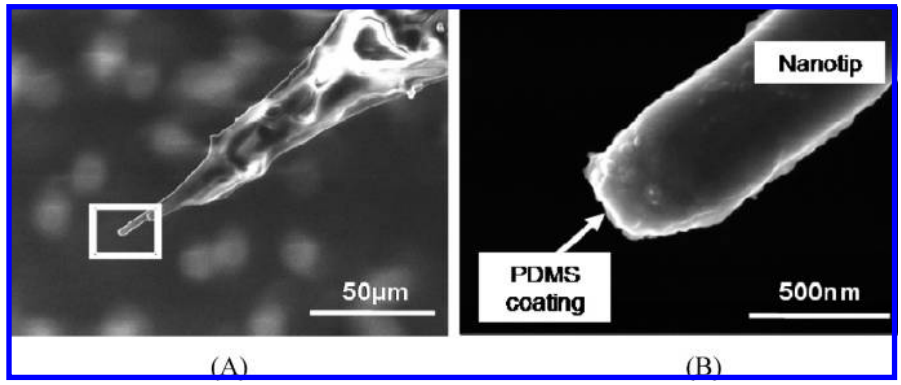

Figure 6. SEM images of a PDMS-coated nanotip. (A) PDMS-coated nanotip having a single SiC nanowire at the end. (B) Exploded view of the nanotip end coated with a 50 nm thick PDMS layer.

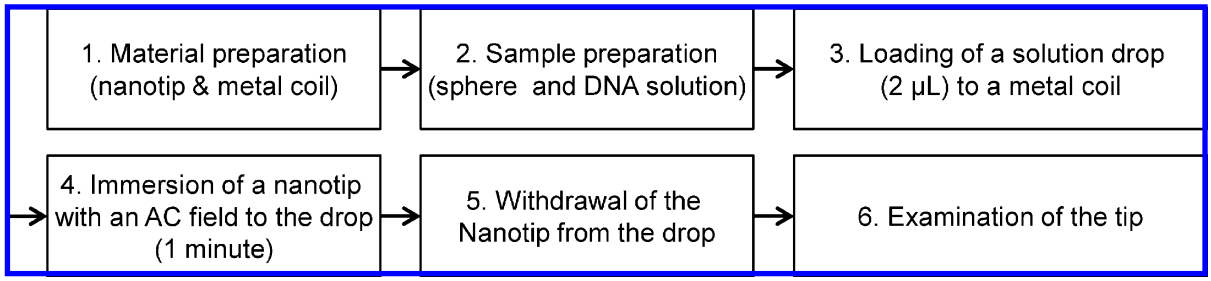

Figure 7. Experimental procedure for capturing nanospheres and DNA using a nanotip.

cence intensity measurements of captured DNA on bare- and PDMS-coated tips.

3.3. Experimental Procedures. ***A. Size-Selective Capture of Polystyrene Spheres.*** To investigate size selectivity using dielectrophoresis and capillary action, fabricated nanotips were used for capturing polystyrene nanospheres. Considering the average diameter (544 ± 141 nm) of the nanotip ends, various sizes of nanospheres were prepared. The average diameters and the standard deviations of polystyrene spheres (Bangs Laboratories, Inc., Fishers, IN) were 100 ± 70, 140 ± 70, 200 ± 70, 300 ± 70, 490 ± 70, 700 ± 70, and 950 ± 70 nm, which were obtained from the supplier's information. The concentration of the spheres dispersed in deionized (DI) water was 10^{11} spheres/mL.

For the nanosphere-capturing experiment, a 2 μL drop of each sphere solution was held in a metal coil as shown in Figure 4(A). The diameter of the coil was 1.5 mm for all experiments. Subsequently, a nanotip without PDMS coating was immersed in the solution drop with the application of 20 V_{pp} at 10 kHz (AC potential). A nanotip without PDMS was used for this experiment but was not reused. The frequency of 10 kHz was chosen because a positive DEP force was induced to polystyrene spheres at this frequency. After 1 min of the immersion time, the tip was withdrawn gently from the solution drop at an average withdrawal rate of 8 μm/s. At this rate, the contact angle between the tip and the solution was not changed under the observation of an optical microscope. After complete withdrawal, the tip end was investigated by an optical microscope and an SEM to examine the diameters of the captured spheres. The whole experimental procedure is shown in Figure 7.

By comparing the diameters of the captured spheres to those of the tips, a critical normalized diameter $[(d_n)_{critical}]$ was measured. Because the diameters of the spheres varied in accordance with the Gaussian distribution, the largest diameter among the captured nanospheres could be compared with the tip diameter to determine $(d_n)_{critical}$. The detailed conditions to determine $(d_n)_{critical}$ from experimental results are described in the Results and Discussion section. In addition, the mixtures of polystyrene spheres having 100 nm and 6 μm in average diameters were used to validate the size selectivity. 6 μm spheres were used because the sphere diameter was analogous to the cell diameters in a biological solution.

B. λ-DNA Concentration from a Pure DNA Solution and a Sample Mixture. To investigate whether DNA could be captured onto a nanotip, λ-DNA (New England BioLabs, Inc. Ipswich, MA) was prepared. The concentration of the initial DNA solution was 500 μg/mL (16 nM, molecular weight: 31.5×10^6 Da) in TRIS EDTA buffer (pH 7.5). To concentrate λ-DNA, a nanotip was dipped in a 2 μL solution drop, which was hung in a metal coil. An AC potential of 20 V_{pp} at 5 MHz was applied to the coil and the nanotip to induce a DEP force. At this frequency, DNA molecules in a buffer solution were polarized and attracted to the nanotip by DEP.[18] After 1 min of the immersion, the nanotip was withdrawn at the rate of 8 μm/s. The captured DNA on the nanotip was investigated by an epi-fluorescence microscope (Olympus BX-41, Olympus America Inc., Melville, NY), an SEM, and an energy dispersive spectrometer (EDS) of the SEM. For the fluorescence observation of DNA captured onto the nanotip, PicoGreen dsDNA reagent (Invitrogen, Carlsbad, CA) was mixed with DNA. The PicoGreen reagent was a green fluorophoric intercalating dye (excitation, ~480 nm; emission, ~520 nm). The mixture of the dye and DNA was used for the capturing experiments. The experimental parameters including the volume of a solution drop, the AC potential, the immersion time, and the withdrawal rate of a tip were consistently applied to all experiments for DNA capturing.

Two kinds of DNA solutions, (1) pure DNA and (2) sample mixture (DNA + Drosophila cells), were prepared in the TRIS EDTA buffer to study the size-specific capture of DNA. The sample mixture was used to demonstrate the size-selective capturing performance of a nanotip from a biological sample

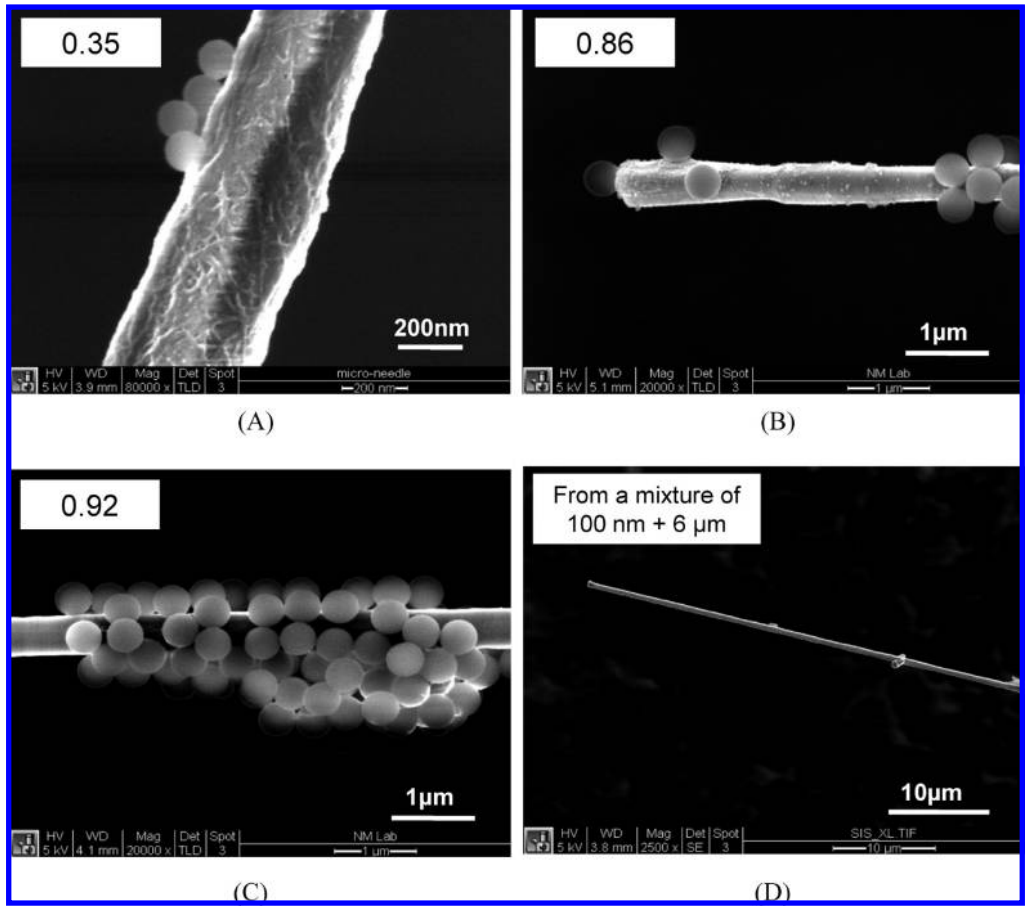

Figure 8. SEM images of the captured nanospheres onto nanotips: each inset shows a maximum normalized diameter. (A) Maximum 125 nm spheres on a 360 nm tip. (B) Maximum 451 nm spheres on a 526 nm tip. (C) Maximum 475 nm spheres on a 514 nm tip. (D) Spheres on a 610 nm nanotip captured from a mixture containing 100 nm and 6 μm spheres in average diameters.

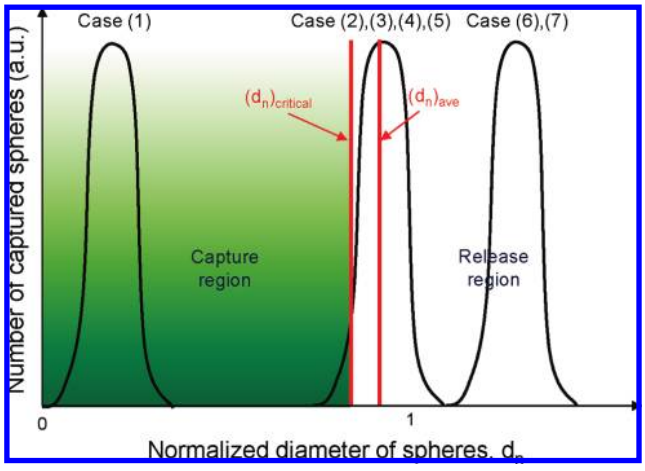

Figure 9. Determination of a critical normalized diameter $[(d_n)_{critical}]$ compared to an averaged normalized diameter $[(d_n)_{ave}]$. The case numbers correspond to the case numbers in Table 1.

containing cells. The performance of a nanotip from a sample mixture was compared to that from a pure sample containing only DNA.

For the pure DNA solution, another λ-DNA solution (initial concentration: 100 μg/mL (3.2 nM), molecular weight: 31.5 $\times$ 10^6 Da, Invitrogen, Carlsbad, CA) was prepared. Various concentrations of λ-DNA were prepared for testing. The prepared concentrations ranged from 1 pg/mL (32 aM) to 1 μg/mL (32 pM) in 10-fold increments with the TRIS EDTA buffer. Subsequently, each DNA solution was mixed with a 200-fold diluted PicoGreen dsDNA reagent in dimethyl sulfoxide (DMSO) with the ratio of 1:1. For the sample mixture solution, the prepared pure λ-DNA solutions were mixed with Drosophila cells (initial concentration: 10^7 cells/mL, Invitrogen, Carlsbad, CA). The mixing ratio of the λ-DNA solutions to the Drosophila cell solution was 2:1, respectively. Therefore, the final DNA concentrations of the mixtures ranged from 0.67 pg/mL (21 aM) to 0.67 μg/mL (21 pM) in 10-fold increments. The concentration of the Drosophila cell solution was uniformly 3.3 $\times$ 10^6 cells/mL in the sample mixture solutions. The Drosophila cells had a spherical morphology with a diameter of 10 μm.[19] Due to the large diameter of the Drosophila cells, the capturing of the cells could be determined by using an optical microscope. After the preparation of the pure DNA and the sample mixture solutions, the capturing experiment was performed by the procedures illustrated in Figure 7. PDMS-coated nanotips were used for these DNA experiments.

After capturing DNA onto a PDMS-coated nanotip, the epi-fluorescence microscope was used to evaluate the fluorescence intensity, which determined the amount of the captured DNA. By using the imaging software, Image J (NIH), the fluorescence intensity in a rectangular area of 23.8 μm $\times$ 4.2 μm was measured at the end of a nanotip. The background fluorescence emission (negative control) was also measured for the same area. The negative control signal was obtained from the solution of a pure PicoGreen reagent without DNA. The measurement of fluorescence emission was repeated three times, and the fluorescence intensities were averaged.

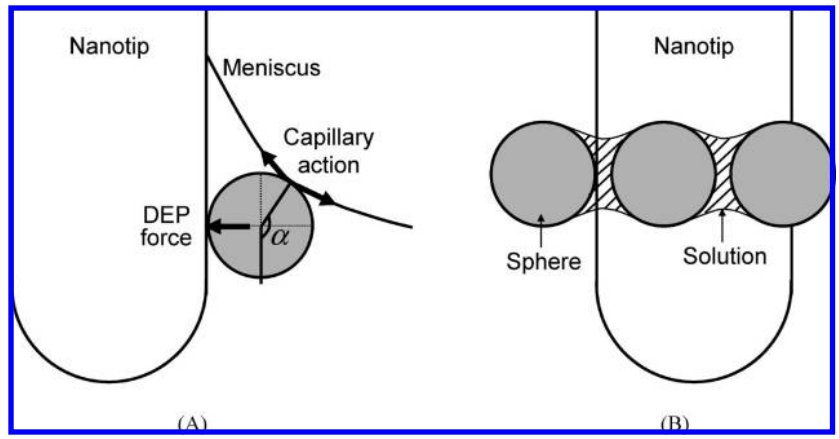

Figure 10. (A) Split angle (α) when a spherical particle is attracted to the side of a tip. (B) Clustering of spheres due to capillary action (multiple particle interaction).

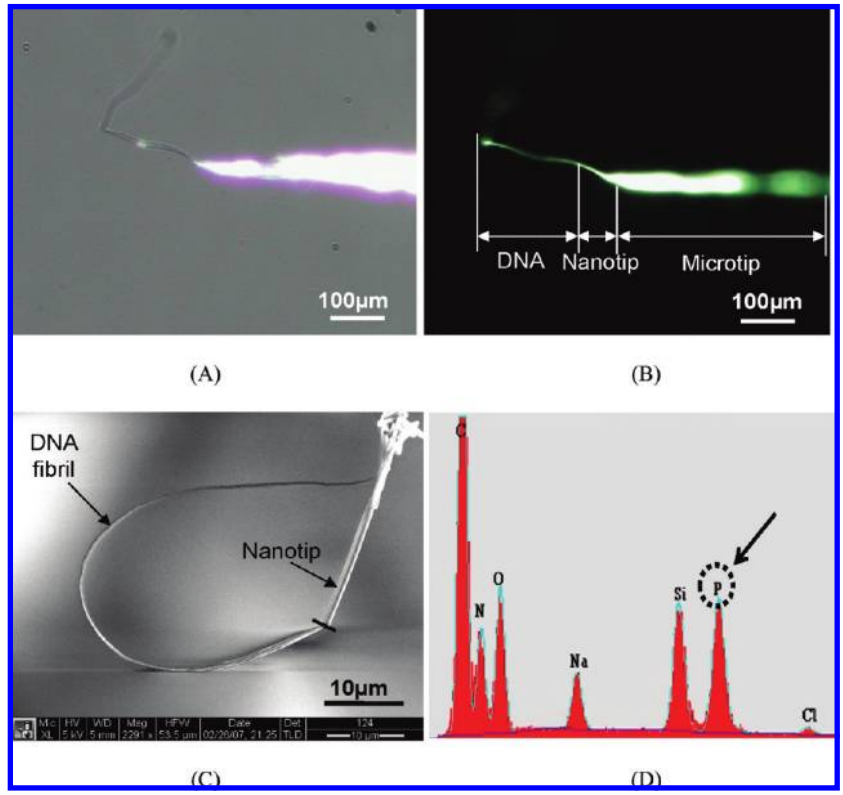

Figure 11. Results of capturing λ-DNA molecules (concentration: 500 μg/mL) using a nanotip. (A) Optical image of a nanotip having a DNA fibril. (B) Corresponding fluorescence image of (A); blurred image at the end shows a vibrating DNA fibril due to air flow. (C) Corresponding SEM image of (A). (D) EDS analysis of the DNA fibril of (C).

Three PDMS-coated nanotips were used for three repetitive experiments. One tip was reused from the lowest concentration to the highest concentration by releasing the captured DNA in boiling DI water for five minutes. This releasing process was repeated three times to clean a used PDMS-coated nanotip. The release of DNA was validated by examination of the tip surface with a fluorescence microscope. Once the fluorescence intensity was measured within the error range of the negative control signal, the tip was then reused to capture DNA of the next higher concentration. The reuse of a nanotip was required because of the variation of a nanotip shape. By reusing the same tip for the six concentrations, the capturing performance could be consistently compared.

4. Results and Discussion

4.1. Size-Selective Capture of Polystyrene Spheres. To study the size selectivity effect caused by dielectrophoresis and capillary action, polystyrene nanospheres were used. The main purpose of the experiment was to validate the presence of the $(d_n)_{critical}$ predicted by theoretical analysis. When a nanotip was immersed in a solution containing nanospheres with an AC potential of 20 V_{pp} at 10 kHz, polystyrene spheres were attracted in the vicinity of the tip by a DEP force. The attracted spheres were captured onto nanotips. Figure 8(A) shows the nanospheres captured from spheres of 100 nm in a nominal diameter (d_{sphere}). The maximum diameter of the captured spheres $[(d_{capture})_{max}]$ is 125 nm, which are captured onto a nanotip having a diameter of 360 nm ($d_{nanotip}$). The maximum normalized diameter, which is the ratio of the maximum sphere diameter to the tip diameter, is 0.35. Figures 8(B) and (C) show that the maximum normalized diameters of the captured spheres are 0.86 and 0.92, respectively. In the experiment for mixing spheres having different diameters

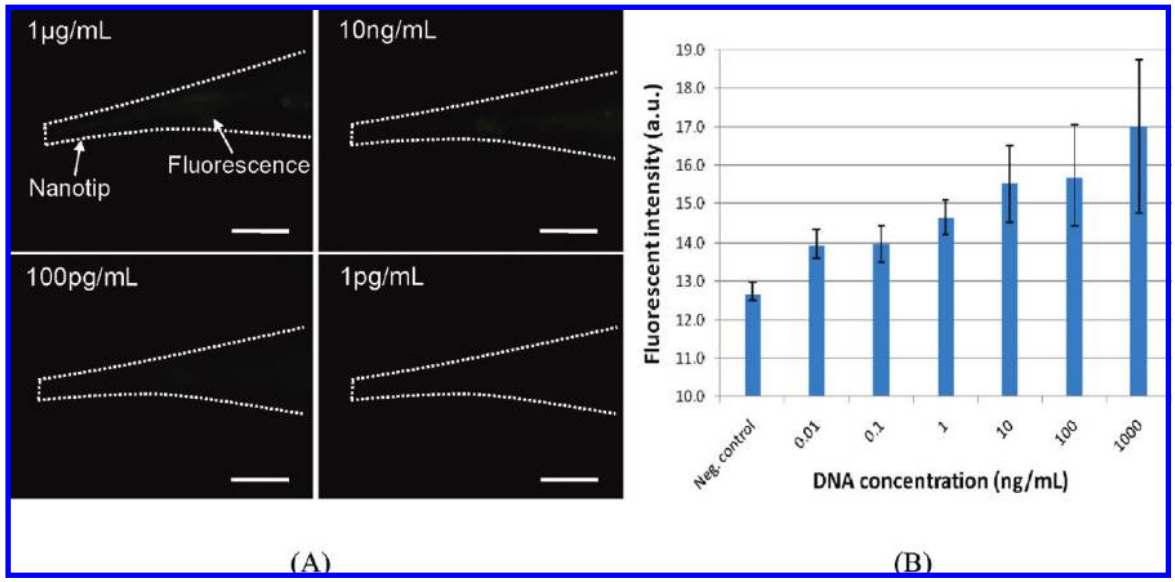

Figure 12. Results of capturing λ-DNA for various DNA concentrations. (A) Fluorescence images for DNA concentrations of 1 μg/mL, 10 ng/mL, 100 pg/mL, and 1 pg/mL (scale bars: 5 μm). Green fluorescence emissions show DNA. (B) Fluorescence intensities vs DNA concentrations. In the graph, the error bars represent the maximum and minimum intensities for three experiments.

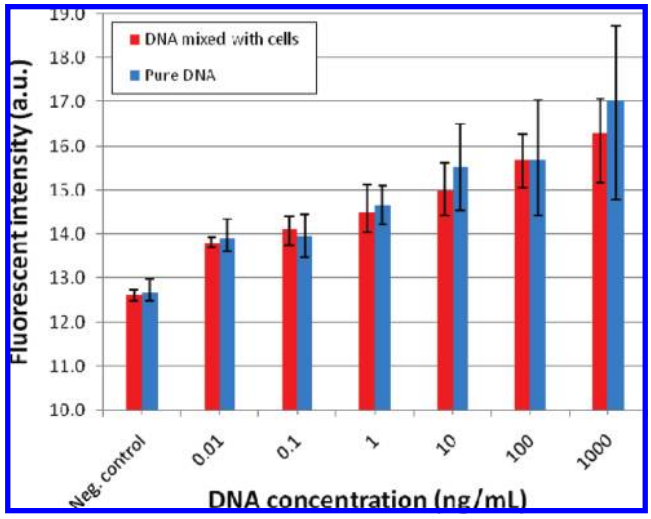

Figure 13. Results of capturing λ-DNA from a sample mixture containing λ-DNA and Drosophila cells. The results are compared with the capturing results from a pure DNA solution. In the graph, the error bars represent the maximum and minimum intensities for three experiments.

(100 nm + 6 μm diameter spheres), only the 100 nm diameter spheres are captured to the nanotip (610 nm in $d_{nanotip}$) due to capillary action [Figure 8(D)].

Table 1 summarizes the capturing results of polystyrene spheres using nanotips. Among the captured spheres onto a nanotip, the largest sphere diameter is normalized by the tip diameter to obtain $(d_n)_{critical}$. According to Table 1, the $(d_n)_{critical}$ is in the range of 0.84 ± 0.07 (average ± standard deviation) using the cases (2), (3), (4), and (5). Other cases are not applicable to this determination of $(d_n)_{critical}$ either when the averaged normalized diameter $[(d_n)_{ave}]$ is much smaller than $(d_n)_{critical}$ such as the case (1) or when spheres are not captured such as the cases (6) and (7). The normalized diameter (d_n) varies according to the Gaussian distribution as illustrated in Figure 9. In the figure, the bell curves show the Gaussian distribution of d_n. When $(d_n)_{ave}$ is slightly greater than $(d_n)_{critical}$ [cases (2), (3), (4), and (5) in Table 1], $(d_n)_{critical}$ is determined by the ratio of the maximum diameter of captured spheres to the nanotip diameter $[(d_{capture})_{max}/d_{nanotip}]$, whereas when $(d_n)_{ave}$ is much smaller than $(d_n)_{critical}$ [cases (1) in Table 1], $(d_n)_{critical}$ cannot be determined because a larger diameter of spheres can be captured. In addition, when spheres are not captured [cases (6) and (7) in Table 1], $(d_n)_{critical}$ cannot be determined. Figure 9 illustrates the capture and release regions with the cases and $(d_n)_{critical}$. In this way, the $(d_n)_{critical}$ using the polystyrene nanospheres was determined in the range of 0.77−0.92 (0.84 ± 0.07). In the mixture experiment of 100 nm and 6 μm spheres, 6 μm spheres could not be captured onto a nanotip because $(d_n)_{ave}$ of 6 μm spheres was much greater than the range of $(d_n)_{critical}$. This result validates the size-selective capturing mechanism of polystyrene spheres using nanotips.

Comparing the $(d_n)_{critical}$ (0.84 ± 0.07) of the experimental results to the $(d_n)_{critical}$ (0.39) of the analytical study, the experimental $(d_n)_{critical}$ is higher than the analytical $(d_n)_{critical}$. This discrepancy can be mainly caused by the DEP force generated from the AC field. Because the DEP force is added to the capturing capillary force, the $(d_n)_{critical}$ is increased. As illustrated in Figure 10(A), the DEP force attracts spheres to the side of a tip as shown in Figure 8. Without the DEP force, the spheres should be pulled to the tip end because the split angle (α) in Figure 10(A) is always greater than 90°. Due to the attractive DEP force, the spheres can be captured to the side of a nanotip.

In addition to the DEP force, the discrepancy of the $(d_n)_{critical}$ between the analytical study and experimental results is caused by the experimental conditions including the tip geometry, the multiple particle interaction, and the contact angle. The sphere at the side of a tip may not be pulled to the end of the tip if the surface of the nanotip is rough or the orientation of the nanotip is not exactly orthogonal to the tangent of a spherical drop during the withdrawal of a tip. In this case, the split angle smaller than 90° can be generated, and thus, the sphere can be captured onto the side of a tip.

When a nanotip is surrounded with a cluster of spheres (multiple particle interaction), the spheres are captured onto the side of the tip as shown in Figure 8(C). The cluster formation around a nanotip is frequently observed during the nanosphere capturing process because the spheres are delivered to the air−liquid−solid interface by capillary action. The delivery of

TABLE 1: Capturing Results of Nanospheres Using Nanotips[a]

	$d_{nanotip}$	d_{sphere}	$(d_n)_{ave} = d_{sphere}/d_{nanotip}$	$(d_{capture})_{max}$	$(d_n)_{critical} = (d_{capture})_{max}/d_{nanotip}$	capturing
(1)	360 nm	100 nm	0.28	125 nm	NA	yes
(2)	595 nm	490 nm	0.82	461 nm	0.77	yes
(3)	347 nm	300 nm	0.86	274 nm	0.79	yes
(4)	526 nm	490 nm	0.93	451 nm	0.86	yes
(5)	514 nm	490 nm	0.95	475 nm	0.92	yes
(6)	623 nm	700 nm	1.12	NA	NA	no
(7)	773 nm	950 nm	1.22	NA	NA	no

[a] $d_{nanotip}$, nanotip diameter; d_{sphere}, nominal diameter of nanospheres from the vendor's information; $(d_n)_{ave}$, averaged normalized diameter $(d_{sphere}/d_{nanotip})$; $(d_{capture})_{max}$, maximum diameter of captured spheres; $(d_n)_{critical}$, critical normalized diameter $[(d_{capture})_{max}/d_{nanotip}]$; and 'NA' means 'not applicable'.

spheres to the interface can be generated by the DEP force in conjunction with evaporation of a solution and the compressive force due to capillary action.[20] As evaporation continues, the capillary action among the attracted spheres can generate a coagulating force [Figure 10(B)]. Therefore, the interactive forces among the delivered spheres can increase the capturing force.

Other than the geometric and the multiple particle interaction effects, the $(d_n)_{critical}$ can be changed due to the contact angle to nanotip surface. The contact angle [θ_1 in Figure 1(B)] at a nanotip can be changed by the surface properties of a tip, the hysteresis, and an electric field (e.g., electro-wetting). Also, molecular interaction forces (e.g., van der Waals force) can be considered, but the molecular force may not be large in liquid compared to the capillary force and the DEP force.[21,22] Therefore, the $(d_n)_{critical}$ should be modified by the specific experimental conditions.

4.2. Size-Specific Capturing of λ-DNA. To investigate whether DNA could be captured by a nanotip, λ-DNA spiked in a TRIS EDTA buffer solution was prepared. Using a nanotip with an AC field, λ-DNA was concentrated onto the tip by dielectrophoresis and capillary action. Figures 11(A), (B), and (C) show the captured λ-DNA molecules on nanotips. Note that the nanotips used for this experiment were not coated with PDMS. Using a DNA concentration of 500 μg/mL, a ~400 μm long DNA fibril was formed at the end of the tip. Due to the high concentration, the molecules formed the fibril by the capillary force when the tip was withdrawn from the solution. Figure 11(A) shows an optical microscope image of the captured DNA onto a nanotip, and Figure 11(B) presents the corresponding fluorescence microscope image. The green emission shows the captured DNA molecules. Figure 11(C) shows the corresponding SEM image of Figure 11(A). The DNA fibril was bent in the SEM vacuum chamber due to the water evaporation and the exposure to the high-energy electron beam.

The EDS analysis of the captured DNA on the tip shows that elements including C, N, O, Na, Si, P, and Cl are detected (acceleration voltage: 10 kV) [Figure 11(D)]. C and Si are the elements from the SiC nanowires and SWCNTs. Na and Cl are present in the buffer solution. The elements of DNA, C, N, O, and P are also detected. In particular, P is a unique element only present in DNA indicated by a black arrow in Figure 11(D). Therefore, the fibril must be composed of DNA. In our further investigation, P was not detected in various control samples including buffer, pure water, fluorescence dye, and bare nanotips.

To compare the DNA capturing performances using a nanotip for pure and mixed samples, DNA molecules having various concentrations were captured to nanotips. The captured DNA was investigated by a fluorescence microscope as shown in Figure 12(A). The concentrations of DNA solutions ranged from 1 pg/mL (32 aM) to 1 μg/mL (32 pM) in 10-fold increments. Figure 12(B) shows the fluorescence intensities according to the various DNA concentrations. The experiment was repeated three times for each DNA concentration. Note that the fluorescence intensities were compared with the negative control signals that were measured with a pure PicoGreen reagent. When the concentration is 1 pg/mL, the intensity from the tip is in the error range of the negative control signals as shown in Figure 12(A). Therefore, the detection limit of the proposed nanotip is 10 pg/mL (320 aM). In the graph of Figure 12(B), error bars are the maximum and minimum intensities from three experiments using three different nanotips. The inconsistent geometry of the nanotips could cause the variations in fluorescence measurement.

To investigate the size-specific capturing of DNA from a sample mixture containing cells, Drosophila cells were mixed with pure λ-DNA molecules in a TRIS EDTA buffer solution. The prepared DNA concentrations were from 0.67 pg/mL (21 aM) to 0.67 μg/mL (21 pM) by 10 folds. In this experiment, the limit of detection based on the fluorescence microscopy is 6.7 pg/mL (210 aM) as shown in Figure 13. DNA molecules were only captured onto a nanotip, while the cells were left in a solution, which demonstrated the size-specific capturing mechanism. Considering the ratio of the normalized diameter of Drosophila cells (10 μm) to an averaged nanotip diameter (544 nm) as 18.4, the ratio was much larger than the range of $(d_n)_{critical}$ (0.84 ± 0.07). Thus, the cells could not be captured onto nanotips. To validate the capture of the cells onto a tip, a microtip having 250 μm in diameter was used to capture the cells. The cells were captured on the microtip using an AC potential (20 V_{pp} @ 5 MHz). In comparison to the fluorescence intensities for the pure and mixed DNA samples, the intensities show a similar trend and the amplitude as shown in Figure 13.

When a nanotip (e.g., ~500 nm in diameter) is applied to concentration of DNA out of a biological sample, nanosized particles including proteins can also be captured because the sizes of proteins are in the order of tens of nanometers. To concentrate purely DNA from a sample mixture, the captured DNA and proteins can be released in a vial and purified by an enzyme dissolving protein. Subsequently, the purified DNA is recaptured by a nanotip with the same mechanism. In spite of this repetition, the proposed method using a nanotip is beneficial in that extracellular DNA is separated from genomic DNA in normal cells. In addition, the rapid concentration using the combination of the DEP and capillary forces is another advantage in that the genetic information of extracellular DNA can be collected without loss or damage of the information, which significantly simplifies the sample preparation steps.

5. Conclusions

For direct concentration of extracellular DNA from a sample mixture, λ-DNA immersed in a solution was prepared and captured onto a nanotip in a size-specific way using dielectrophoresis and capillary action. A critical normalized diameter $[(d_n)_{critical}]$, which was estimated by an analytical model, was presented to determine the capture of certain range diameters of polystyrene nanospheres using a nanotip. In the experiment, $(d_n)_{critical}$ was determined in the range of 0.84 ± 0.07. When the size-specific concentration mechanism was used for DNA capture, λ-DNA molecules were size-selectively captured onto a nanotip from a sample mixture containing Drosophila cells and λ-DNA. The captured DNA was investigated using SEM, X-ray, and fluorescence microscopy. The results from the investigation suggest that the detection limit for λ-DNA using a nanotip technique is 6.7 pg/mL (210 aM). The presented size-specific concentration mechanism demonstrates a potential to directly concentrate extracellular DNA from a raw or minimally treated sample.

Acknowledgment. The support of NSF STTR PHASE I grant (award number: IIP 0740525) of 'Nano-Needle DNA Biosensor for In-Situ Direct Detection' (Program manager: Dr. Muralidharan S. Nair) is gratefully acknowledged.

References and Notes

(1) Gormally, E.; Caboux, E.; Vineis, P.; Hainaut, P. *Mutat. Res., Rev. Mutat. Res.* **2007**, *635*, 105.

(2) Vlassov, V. V.; Laktionov, P. P.; Rykova, E. Y. *Bioessays* **2007**, *29*, 654.

(3) Cotner, J. B.; Ogdahl, M. L.; Biddanda, B. A. *Aquat. Microb. Ecol.* **2001**, *25*, 65.

(4) Siuda, W.; Chrost, R. J.; Gude, H. *Aquat. Microb. Ecol.* **1998**, *15*, 89.

(5) Siuda, W.; Chrost, R. J. *Aquat. Microb. Ecol.* **2000**, *21*, 195.

(6) Zhu, B. *Water Res.* **2006**, *40*, 3231.

(7) Rutjes, S. A.; Italiaander, R.; van den Berg, H.; Lodder, W. J.; Husman, A. M. D. *Appl. Environ. Microbiol.* **2005**, *71*, 3734.

(8) Maruyama, F.; Tani, K.; Kenzaka, T.; Yamaguchi, N.; Nasu, M. *Appl. Environ. Microbiol.* **2006**, *72*, 6248.

(9) Jones, T. B. *Electromechanics of particles*; Cambridge University Press: New York, 1995.

(10) Liu, Y.; Liu, W. K.; Belytschko, T.; Patankar, N.; To, A. C.; Kopacz, A.; Chung, J. H. *Int. J. Numer. Methods Eng.* **2007**, *71*, 379.

(11) Liu, Y.; Chung, J. H.; Liu, W. K.; Ruoff, R. S. *J. Phys. Chem. B* **2006**, *110*, 14098.

(12) Rao, N. N. *Basic electromagnetics with applications*; Prentice-Hall: Englewood Cliffs, NJ, 1972.

(13) Tretinnikov, O. N. *Langmuir* **2000**, *16*, 2751.

(14) Zhmud, B.; Tiberg, F. *Adv. Colloid Interface Sci.* **2005**, *113*, 21.

(15) Hans-Jürgen Butt, K. G.; Kappl M. *Physics and Chemistry of Interfaces*; Wiley-VCH: Weinheim, Germany, 2003.

(16) Hotta, K.; Takeda, K.; Iinoya, K. *Powder Technol.* **1974**, *10*, 231.

(17) Tang, J.; Gao, B.; Geng, H. Z.; Velev, O. D.; Qin, L. C.; Zhou, O. *Adv. Mater.* **2003**, *15*, 1352.

(18) Tuukkanen, S.; Kuzyk, A.; Toppari, J. J.; Hakkinen, H.; Hytonen, V. P.; Niskanen, E.; Rinkio, M.; Torma, P. *Nanotechnology* **2007**, *18*, 10.

(19) Rogers, S. L.; Wiedemann, U.; Stuurman, N.; Vale, R. D. *J. Cell Biol.* **2003**, *162*, 1079.

(20) Liu, Y. L.; Oh, K.; Bai, J. G.; Chang, C. L.; Yeo, W.; Chung, J. H.; Lee, K. H.; Liu, W. K. *Comput. Methods Appl. Mech. Eng.* **2008**, *197*, 2156.

(21) Wei, Z.; Zhao, Y. P. *J. Phys. D, Appl. Phys.* **2007**, *40*, 4368.

(22) Paajanen, M.; Katainen, J.; Pakarinen, O. H.; Foster, A. S.; Lahtinen, J. *J. Colloid Interface Sci.* **2006**, *304*, 518.

JP900618T